promoter (part 1), *Bull. J.S.M.E.* **29**(258), 4228–4234 (1986).
3. Y. Utaka, A. Saito and H. Yanagida, On the mechanism determining the transition mode from dropwise to film condensation, *Int. J. Heat Mass Transfer* **31**, 1113–1120 (1988).
4. Y. Utaka, A. Saito, T. Tani, H. Shibuya and K. Katayama, Study on dropwise condensation curves (measurement of propylene glycol vapor on PTFE coated surface), *Bull. J.S.M.E.* **28**(240), 1150–1157 (1985).
5. S. A. Stylianous and J. W. Rose, Drop-to-filmwise condensation transition: heat transfer measurement for ethanediol, *Int. J. Heat Mass Transfer* **26**, 747–760 (1983).
6. E. K. Kalinin, I. I. Berlin and V. V. Kostiouk, Transition boiling heat transfer, *Adv. Heat Transfer* **18**, 214–323 (1987).
7. P. T. Saunders, *An Introduction to Catastrophe Theory*. Cambridge University Press, Cambridge (1980).
8. F. H. Ling, Catastrophe theory—history, current situation and future, *Adv. Mech.* **14**(4), 389–404 (1984) (in Chinese).
9. R. Ito, Application of catastrophe theory to the breakup of a liquid drop in a shear field, *Int. Chem. Engng* **20**(2), 266–271 (1980).
10. C. E. Lacy, M. Sheintuch and A. E. Dukler, Methods of deterministic chaos applied to the flow of thin wavy films, *A.I.Ch.E. Jl* **37**(4), 481–489 (1991).
11. J. L. Moiola, A. Desages and J. Romagnoli, Degenerate Hopf bifurcations via feedback system theory: higher-order harmonic balance, *Chem. Engng Sci.* **46**(5/6), 1475–1491 (1991).
12. A. Kienle and W. Marouardt, Bifurcation analysis and steady-state multiplicity of multicomponent, nonequilibrium distillation processes, *Chem. Engng Sci.* **46**(7), 1757–1769 (1991).
13. A. A. Berezin, Application of catastrophe theory to phase transition of trapped particles, *Physica Scripta* **43**, 111–115 (1991).
14. J. A. Gaite, Phase transitions as catastrophes: the tricritical point, *Phy. Res.* **41**(10), 3520–3524 (1990).
15. I. Tanasawa, Advances in condensation heat transfer, *Adv. Heat Transfer* **21**, 55–139 (1991).
16. A. Majthay, *Foundations of Catastrophe Theory*. Pitman, Carthage, Illinois (1985).
17. D. Q. Xu and J. F. Lin, Nucleate boiling and CHF of ether, acetone, carbon tetrachloride and ethyl alcohol, *Rep. Inst. Chem. Engng*, Dalian University of Technology (1965).

Pergamon

Int. J. Heat Mass Transfer. Vol. 37, No. 3, pp. 535–539, 1994

0017-9310/94 $6.00 + 0.00

Constant flux, turbulent convection data using infrared imaging

A. H. W. Lee, D. E. Klein and J. P. Lamb
Department of Mechanical Engineering, The University of Texas at Austin, Austin, TX 78712, U.S.A.

(*Received* 26 *May* 1992 *and in final form* 22 *March* 1993)

INTRODUCTION

In recent years, the infrared (IR) imaging system has proven to be a powerful experimental tool for surface temperature mapping. This system has the advantage of being non-invasive, thus allowing measurements without interfering with the phenomenon under investigation. It also maps continuously the entire region of interest. The output can be displayed on a video screen, thus permitting real-time evaluation of the results [1]. It is believed that the IR imaging technique is as accurate as conventional thermocouples. Some recent applications of this technique in heat transfer include investigation of aerodynamic heating [2] and the detection of transition in a boundary layer flow [3].

This paper describes a recent study which obtained convection data using an IR imaging system in flow past a smooth surface. Since this study was carried out as an initial step in obtaining data for flow past roughened surfaces [4], friction factors were also determined. The project included the design and construction of a smooth test surface capable of providing uniform heat flux using electrically heated foils. Experimental data included surface temperature variation, pressure gradients, and mean velocity profiles. The data were analyzed and compared with numerical solutions.

EXPERIMENTAL FACILITIES

Experiments were conducted in an adjustable-height wind tunnel driven by a 74.6 kW fan. The discharge vent of the fan was 1.11 m wide and 0.93 m high. A transition section reduced the height to 0.38 m while the width remained the same at 1.11 m. The variable geometry section of the tunnel was 14.6 m long and 1.11 m wide. Its height could be varied from 5.1 to 38 cm, thus allowing operations at different hydraulic diameters. However, operation at a height less than 15 cm was found to be unsatisfactory due to mechanical vibration. The test section of the tunnel was 2.44 m long. A 3.35 m long diffuser region was located immediately downstream of the test section. The diffuser served to prevent end effects from being propagated upstream into the test section. The smooth test plate was 1.83 m long and 1.91 cm thick. It was constructed of birch which reduced heat losses due to conduction. To further minimize heat losses, the test plate was bonded with RTV silicone between two pieces of insulator IV3 Polyurethane, each 0.32 cm thick.

Uniform heating on the test surface was provided by 85 electrically heated metal strips which were glued to the top surface of the insulator with 3M two-part Epoxy. The metal strips, made of Type 302 Stainless Steel 2.0 cm wide, 0.0025 cm thick were spaced 0.1 cm apart. The heater strips on the test surface were divided into five sections of equal surface area. Each section consisted of 17 heater strips connected by copper bus bars attached to the sides of the test plate. Each heater section was connected to a 230 V, 6 A DC power supply having a maximum output of 700 W m^{-2}. To improve the thermal imaging process, a 32 cm width along the center line of the test plate was sprayed with black enamel paint to maximize thermal radiation.

Pressure taps along the top wall of the wind tunnel, including four taps in the test section, were used to measure wall pressure distributions. Velocity profiles were measured using a 32 cm pitot-static tube located about 35.5 cm upstream from the end of the test section. The vertical position of the probe was controlled by a Compumotor with increments varying from 0.5 to 1.3 cm and an accuracy of 0.025 cm.

The data acquisition system used in the present study consisted of an IBM XT computer, a Keithley Model 706

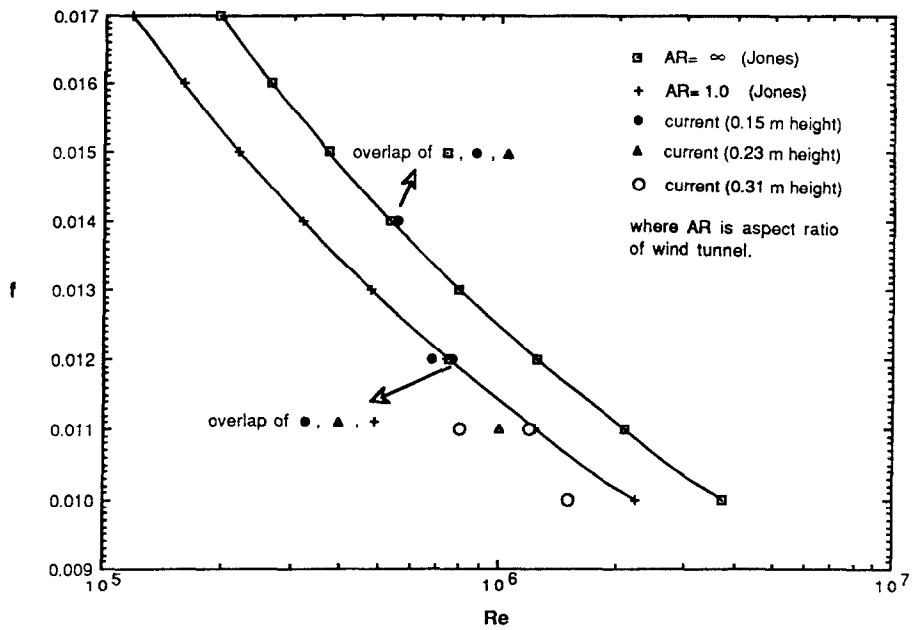

FIG. 1. Friction factor vs Reynolds number for three wind tunnel heights. (Reynolds number based on average velocity and hydraulic diameter.)

Scanner, and a Keithley Model 193 Multimeter. Surface temperatures were measured with an Inframetrics Model 600L IR Imaging Radiometer. The system was calibrated to operate in the 8 to 12 μm IR waveband. The IR camera had a Mercury–Cadmium–Telluride detector with a specified time constant of 0.5–1 μs. This IR detector has a square shape of length 0.025 mm and is cooled to 77 K by a closed cycle microcooler which operates on a Sterling cycle. Unlike IR cameras that use liquid nitrogen cooling, the model 600L can operate continuously and can be positioned at any angle with respect to the target surface.

The field of view of the IR camera was $20° \times 15°$. The thermal resolution is specified according to either of two parameters: NETD or MDTD. The Noise Equivalent Temperature Difference is defined as the temperature difference which produces a change in signal output equal to the system r.m.s. noise. The NETD in the system at 30° was less than 0.2°C. The Minimum Detectable Temperature Difference performance criterion indicated a value of 0.1°C at a surface temperature of 30°C.

Calibration tests were performed to determine the accuracy, spatial resolution, emittance variation, response to temperature gradients, and effect of surroundings on the infrared measurements. Additional information on these calibration tests is found in ref. [4].

EXPERIMENTAL INVESTIGATION AND RESULTS

Static pressure measurements

Experimental tests without heat transfer were conducted to measure static pressures along the centerline of the wind tunnel. Such measurements along the wind tunnel were essential to obtain the wall friction coefficients. The friction data were used to ensure that a fully developed flow condition existed in the test section. Twenty-eight static taps on the centerline of the roof of the wind tunnel were used for the static pressure drop measurements. Each static tap was of 0.08 cm diameter. Plastic tubing was used to connect each static tap to a port on the scanivalve.

It was found that the static pressure distributions were essentially linear for that portion of the wind tunnel 6.1 m downstream from the entrance. This result was consistent even for a wind tunnel height of 30.5 cm (hydraulic diameter 47.8 cm) and showed that the entrance length was about 13 hydraulic diameters.

Experimental friction factors were calculated from the following expression:

$$\mathrm{d}p/\mathrm{d}x = (4f\rho\bar{u}^2)/2D_h \qquad (1)$$

where $\bar{u}$ is the axial mean velocity of flow, obtained by integrating the velocity profiles. A mean or effective value of

Table 1. Conditions at which friction and forced convection data were obtained

Wind tunnel height (m)	Centerline velocity ($m\,s^{-1}$)	Reynolds number ($\times 10^6$)	Symbolic notation for velocity	Total heat flux input ($W\,m^{-2}$)	Symbolic notation for heat flux
0.15	32.3	0.55	Low	530	Low
	39.7	0.68	Medium		—
	45.2	0.77	High	3500	High
0.23	31.2	0.75	Low		
	42.8	1.0	Medium		
	50.5	1.2	High		
0.31	26.2	0.80	Low	530	Low
	39.2	1.2	Medium		—
	51.3	1.5	High	3500	High

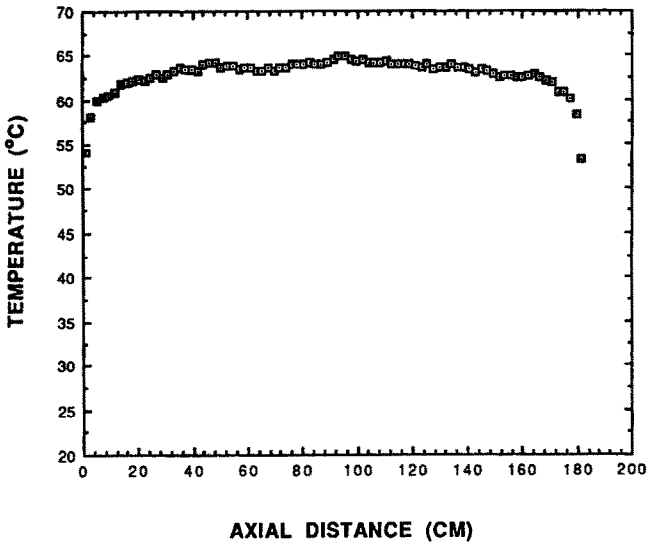

FIG. 2. Experimental free convection temperature distribution on the plate for an average plate temperature of 63°C.

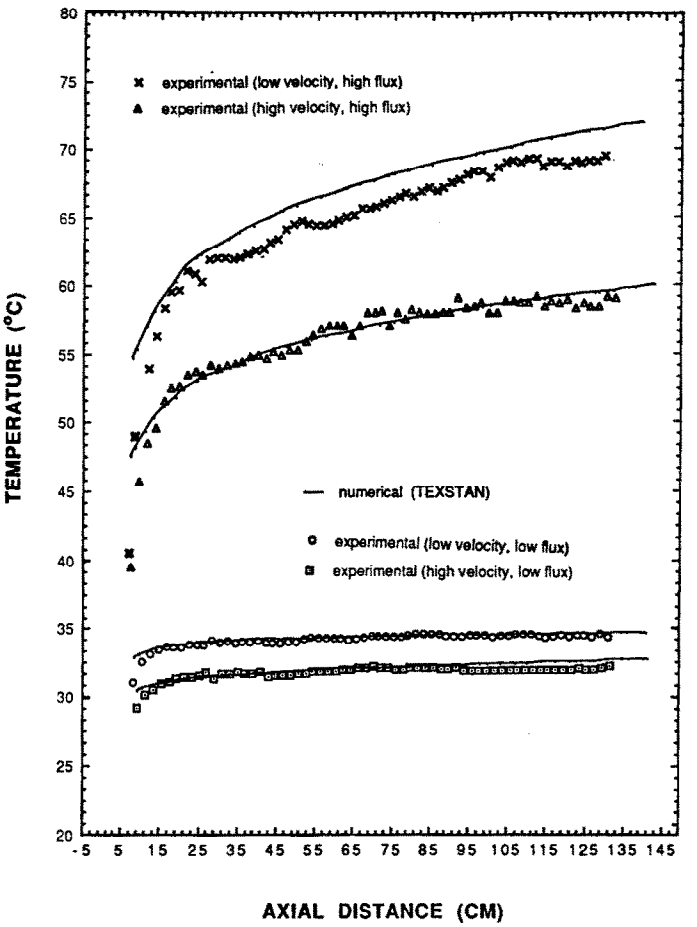

FIG. 3. Forced convection temperature distribution on the plate for 15 cm wind tunnel height.

dp/dx was found from the slope of a least squares line calculated from the experimental data.

Experimental friction factors were calculated using the average velocity values determined by profile integration (discussed in the next section). Figure 1 shows the variation of friction factors with Reynolds number for three wind tunnel heights. For each wind tunnel height, the friction factor decreases with increasing Reynolds number as would be

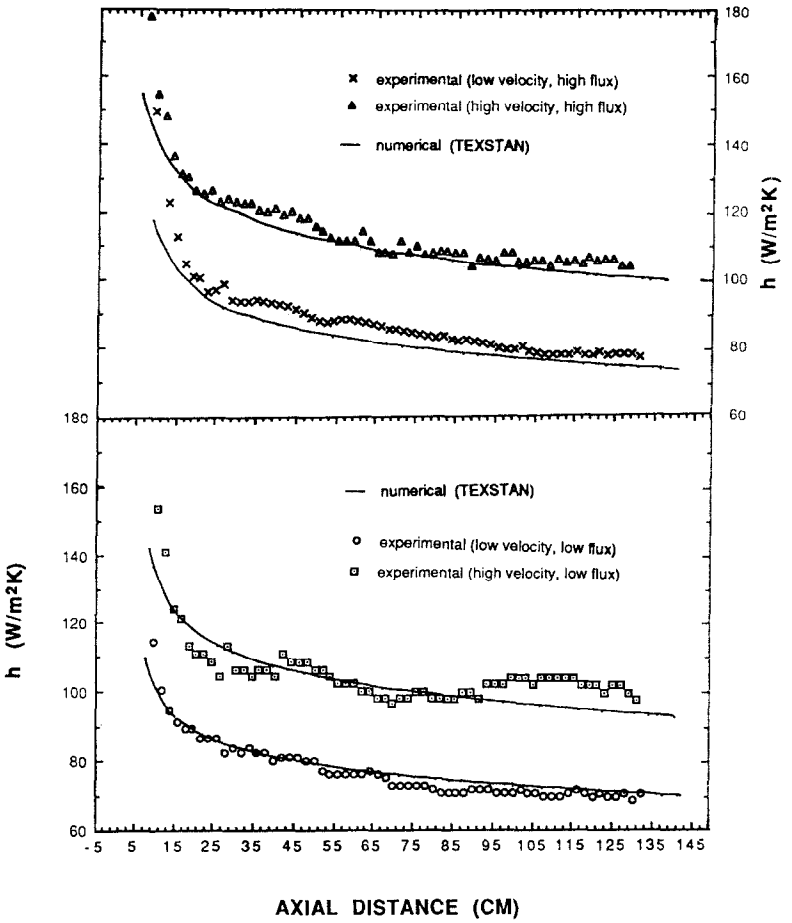

FIG. 4. Forced convection heat transfer coefficient along the plate for 15 cm wind tunnel height.

expected. It was also observed that for a constant Reynolds number, the friction factor increases as the aspect ratio increases. This result is consistent with the theoretical findings of Hartnett *et al.* [5] and Jones [6].

Velocity profile measurements

In order to verify two-dimensional flow in the test section, velocity profiles at a station 35.5 cm upstream from the trailing edge of the test plate were measured for all flow conditions tabulated in Table 1. Within the limits of experimental error, there was good symmetry of flow about the centerline for all flow conditions.

The experimental data were found to be in close agreement with the universal law of the wall for flow through smooth surfaces:

$$u^+ = 2.5 \ln y^+ + 5.5. \quad (2)$$

The experimental data for each wind tunnel height yielded an average slope of 2.6 and an average intercept of 5.8. The discrepancy was due to errors in determining the y-location of the probe with sufficient accuracy.

Free convection test

The purpose of these tests was to determine that the heating foils were in proper working condition. The upper portion of the variable geometry section of the tunnel was first lifted about two feet above the test plate in order to allow free air circulation around the heated test plate. Power was then supplied to the stainless steel heating foils without any flow through the tunnel.

Free convection tests were performed for different plate temperatures which were obtained by varying input power to the heating foils (each power supply at the same setting). The IR camera was set to read temperatures in the middle of each heater strip. Figure 2 shows the temperature distributions on the test plate for a nominal plate temperature of 63°C. It is observed that the temperatures were nearly constant over the test plate. All data points were within a range of 3% from the mean value. Plate temperatures at the leading and trailing edges were somewhat lower than the rest of the plate, as one would expect. This was attributed to the augmented natural convection at the edges.

Forced convection tests

The purpose of these tests was to determine that the entire experimental assembly, including the IR thermal camera, was capable of producing reliable heat transfer results. Conditions under which forced convection tests were performed are presented in Table 1. This paper presents the experimental results for flow conditions at a wind tunnel height of 0.15 m. Additional results can be found in ref. [7]. A numerical simulation for each forced convection experiment was also performed, using the computer code TEXSTAN [8]. For each forced convection test, only the distribution of the surface plate temperature was measured, since the heat flux was assumed uniform. Figure 3 shows the temperature distributions along the test plate for cases designated as low and high velocity with low and high heat flux. It is observed that there was good agreement between the numerical and experimental results. For all cases, there was some dis-

agreement near the front edge of the test plate. Since the front edge was adiabatic, one would expect the experimental distribution to display a nearly infinite slope at this point. Generally, the numerical simulations were unable to produce such steep slopes.

The total heat losses due to radiation and conduction (to the bottom of the plate) were estimated to be about 6% each of the total heat input to the test plate. Hence, the experimental heat transfer coefficient was calculated using the equation:

$$h = q''/(T_w - T_m) \tag{3}$$

where q'' was 0.94 of the total electrical power input to the plate (based on a 6% heat loss). In the above equation, the heat flux, q'', and the wall temperature, T_w, were obtained experimentally. However, the bulk temperature of the fluid, T_m, was determined by a heat balance across the test section of the wind tunnel.

Convective heat transfer coefficients from the numerical and experimental results were also compared as shown in Figure 4. Again, there was good agreement between the experimental and numerical results except at the leading edge. Hence, the above results showed that the IR thermal camera was capable of producing a high density of experimental measurements of surface temperatures which exhibit the proper distributions.

CONCLUSIONS

The primary purpose of this study was to obtain convection data using an IR imaging system in flow past smooth surfaces. This study was carried out as an initial step in obtaining data for turbulent flow past discrete roughness. As such, friction factors were also determined. The experimental profiles for both the temperature and heat fluxes were compared to numerical solutions. It was found that there was good agreement between the experimental and numerical results. Hence, the entire experimental assembly, including the IR camera was capable of producing constant heat flux convection data which is consistent with numerical predictions in flow past smooth surfaces. Thus, there is confidence that the apparatus would also yield data of high quality for rough surfaces.

REFERENCES

1. E. Gartenberg, A. S. Roberts and G. V. Selby, Infrared surface imaging as a flowfield diagnostic tool, *Proceedings of the 12th International Congress on Instrumentation in Aerospace Simulation Facilities*, College of William and Mary, Williamsburg, Virginia, 22–25 June (1987).
2. A. M. Bouchardy and G. Durand, Processing of the infrared thermal images for aerodynamic research, *Society of Photo-Optical Instrumentation Engineers International Technical Conference*, Geneva (1983).
3. A. Quast, Detection of transition by infrared image technique, *Proceedings of the 12th International Congress on Instrumentation in Aerospace Simulation Facilities*, College of William and Mary, Williamsburg, Virginia, 22–25 June (1987).
4. D. A. Aliaga, Experimental measurements of local heat transfer coefficients over discrete roughened plates using infrared thermography, Ph.D. Dissertation, The University of Texas at Austin, Texas (1992).
5. J. P. Hartnett, J. C. Y. Koh and S. T. McComas, A comparison of predicted and measured friction factors for turbulent flow through rectangular ducts, *J. Heat Transfer* **84,** 82–88 (1962).
6. O. C. Jones, An improvement in the calculations of turbulent friction in rectangular ducts, *J. Fluids Engng* **98,** 178 (1976).
7. A. H. W. Lee, Experimental investigation of heat transfer and friction in flow past smooth surfaces, M.S. Thesis, The University of Texas at Austin, Texas (1991).
8. J. R. Pietrzyk and M. E. Crawford, A numerical investigation of turbulent mixed convection in vertical annular channels, M.S. Thesis, The University of Texas at Austin, Texas (1985).